Optimized absorption of solar radiations in nano-structured thin films of crystalline silicon via a genetic algorithm

Mayer, Alexandre; Muller, Jérôme; Herman, Aline; Deparis, Olivier

Published in:
Proceedings of SPIE

DOI:
10.1117/12.2185672

Publication date:
2015

Document Version
Publisher's PDF, also known as Version of record

Optimized absorption of solar radiations in nano-structured thin films of crystalline silicon via a genetic algorithm

Alexandre Mayer, Jérôme Muller, Aline Herman and Olivier Deparis

Laboratoire de Physique du Solide, University of Namur,
Rue de Bruxelles 61, 5000 Namur, Belgium

ABSTRACT

We developed a genetic algorithm to achieve optimal absorption of solar radiation in nano-structured thin films of crystalline silicon (c-Si) for applications in photovoltaics. The device includes on the front side a periodic array of inverted pyramids, with conformal passivation layer (a-Si:H or AlO_x) and anti-reflection coating (SiN_x). The device also includes on the back side a passivation layer (a-Si:H) and a flat reflector (ITO and Ag). The geometrical parameters of the inverted pyramids as well as the thickness of the different layers must be adjusted in order to maximize the absorption of solar radiations in the c-Si. The genetic algorithm enables the determination of optimal solutions that lead to high performances by evaluating only a reduced number of parameter combinations. The results achieved by the genetic algorithm for a 40-μm thick c-Si lead to short-circuit currents of 37 mA/cm^2 when a-Si:H is used for the front-side passivation and 39.1 mA/cm^2 when transparent AlO_x is used instead.

Keywords: genetic algorithm, optimization, photovoltaics, solar cell, silicon thin film, nano-texturation, light trapping, super-absorption, RCWA

1. INTRODUCTION

The photovoltaics (PV) market is currently dominated by technologies based on silicon.[1,2] This material is indeed abundant and non toxic. It absorbs the majority of the solar spectrum up to 1200 μm. Commercial PV modules work with crystalline silicon wafers, whose thickness lies typically above 150 μm. When working with thin films of silicon (thickness below 50 μm), one must develop strategies to maintain high absorption of the solar radiation. Texturing the thin film will induce light trapping mechanisms, which compensate indeed for the reduced thickness of c-Si.[3–10] Typical PV modules have an anti-reflection coating (ARC)[11,12] on the front-side in order to reduce reflections of the incident radiation by the device as well as a back reflector (BR) on the rear side in order to prevent this radiation from escaping the crystalline silicon.[4,6] Any light that is not absorbed in the crystalline silicon is indeed lost for the generation of electron-hole pairs. In order to reach high performances, the geometrical characteristics of the front-side texturation as well as the thickness of the different layers that constitute the ARC and the BR must be carefully adjusted.

A systematic exploration of all parameter combinations would lead to computation times that grow exponentially with the number of parameters to be determined. Genetic Algorithms (GA) provide a more efficient approach to this optimization problem.[13–19] The idea consists in working with a population of individuals, each individual being representative of a given set of parameters. The best individuals are selected. They generate new individuals for the next generation. Random mutations are finally introduced in the coding of parameters. When repeated from generation to generation, this evolutionary strategy makes it possible to determine globally optimal solutions.

For problems that involve significant computation times for each evaluation of the objective function we seek at optimizing, it is desirable to solve the problem ideally by a single run of the genetic algorithm. Different

Further author information: (Send correspondence to A.M.)
A.M.: E-mail: alexandre.mayer@unamur.be, Telephone: 32 81 724720
J.M.: E-mail: jerome.muller@unamur.be
A.H.: E-mail: aline.herman@unamur.be
O.D.: E-mail: olivier.deparis@unamur.be

Active Photonic Materials VII, edited by Ganapathi S. Subramania, Stavroula Foteinopoulou, Proc. of SPIE
Vol. 9546, 95461N · © 2015 SPIE · CCC code: 0277-786X/15/$18 · doi: 10.1117/12.2185672

heuristics are therefore implemented in order to reduce the chance of a bad run (GA converging to a local optimum that performs poorly compared to the global optimum). It is also useful to implement heuristics that help the GA finalize the optimization more rapidly, once the good spot has been identified. This is done by making regularly an analysis of the data collected by the GA in order to infer the final solution. The genetic algorithm we developed in this perspective is presented in Sec. II. In Sec. III, we use the genetic algorithm to optimize the absorption of solar radiation in a thin film (40 μm) of crystalline silicon for applications in photovoltaics. Sec. IV finally concludes this work.

2. DESCRIPTION OF THE GENETIC ALGORITHM

Let $f = f(\vec{x})$ be an objective function of n physical parameters x_i, where $x_i \in [x_i^{\min}, x_i^{\max}]$ with a specified granularity of Δx_i in the representation of each parameter. We want to find, amongst the set of all possible parameter combinations, the values of x_i that maximize globally the objective function f.

Each parameter x_i is represented by a string of n_i bits (0 or 1), also called a "gene". The length n_i of each gene is chosen so that $(x_i^{\max} - x_i^{\min})/(2^{n_i} - 1) \leq \Delta x_i$. The value of the physical parameter x_i is then given by $x_i = x_i^{\min} + \langle \text{gene } i \rangle \times \Delta x_i$, where $\langle \text{gene } i \rangle \in [0, 2^{n_i} - 1]$ stands for the value coded by the gene i in Gray binary coding.[16] The genetic algorithm must reject gene values that lead to $x_i > x_i^{\max}$.[19] A given set of physical parameters $\{x_i\}_{i=1}^n$ is finally represented by the juxtaposition of the n genes used for the representation of each parameter. These strings of n genes are also called "DNA".

We work with a population of n_{pop}=100 individuals. Each individual has its own DNA. It is therefore representative of a given set of physical parameters $\{x_i\}_{i=1}^n$. The initial population consists of random individuals. These individuals must be evaluated in order to determine their "fitness". The fitness is taken in this context as the value of the objective function f. The individuals are then sorted according to their fitness.

The bottom n_{rand} individuals of the population are replaced by random individuals. This enables the introduction of seeds to the global optimum that may have been missing in the initial population. The evaluation of these random individuals is actually postponed to the next generation. The next bottom n_{rec} individuals of the current population are replaced by individuals for which the fitness has already been calculated. This recycling is implemented by a rank-based roulette wheel selection applied on a record that contains the whole list of individuals for which the fitness has already been evaluated. This recycling aims at giving a second chance to individuals that may have been discarded too quickly and whose genes may be useful at the current stage of the algorithm. This is done at virtually no additional cost since their fitness has already been calculated. These n_{rec} individuals will participate to the steps of selection, crossover and mutation, which determine the remaining $N = n_{\text{pop}} - n_{\text{rand}}$ individuals of the next generation.

The main core of the genetic algorithm consists then in selecting N individuals ("the parents") amongst the N individuals of the current population for which the fitness is available. A given individual can be selected several times. This selection is achieved by a rank-based roulette wheel selection applied on these N individuals.[16–18] The probability for an individual to be selected by this scheme is proportional to its weight on a "wheel". The best individual receives a weight of N, the second-best a weight of $N - 1$, etc. Individuals with a higher fitness have thus more chance to be selected. For any pair of parents, we determine two "children" for the next generation. These children are obtained either (i) by a one-point crossover of the parents' DNA (probability of 70%), or (ii) by a simple replication of the parents' DNA (probability of 30%). The position in the chain of bits at which the two parts of the parents' DNA is exchanged is chosen randomly.[16–18] The rate of crossover (70%) actually controls a balance between the conservation of good solutions (unchanged individuals transferred to the next generation) and the exploration of new solutions obtained by crossing the parents' DNA. Random mutations are finally introduced in the DNA of the children obtained by crossover. Each bit of their DNA has then a probability of 1% to be reversed. These mutations constitute another driving force for the exploration of parameters.

These steps are repeated from generation to generation until the population finally converges to an optimum of the objective function. Elitism is implemented in order to make sure that the best individual is not lost when going from one generation to the next. Every five generations, the data collected by the genetic algorithm is analyzed in an attempt to anticipate the final solution (see Appendix A). This aims at reducing the time

required by a typical GA to finalize the optimization. The dynamics of the GA can be monitored by representing generation after generation the best and average fitness in the population (f_{best} and f_{mean}) as well as the genetic similarity (s). The genetic similarity represents the fraction of the bits in the population whose value is the same as for the best individual.[16,19] A regular dynamics is characterized by s values raising progressively from 0.5 (random initial population) to 1 (population fully dominated by the best individual). A progress indicator $p = |s - 0.5|/0.5$ is actually defined from s, which in turn specifies n_{rand} and n_{rec} by $n_{\text{rand}} = 0.1 \times n_{\text{pop}} \times (1 - p)$ and $n_{\text{rec}} = 0.05 \times n_{\text{pop}} \times (1 - p)$. This makes the injection of random individuals and the recycling of solutions vanish when the algorithm enters a phase of refinement of the solution ($s \to 1$).[19]

This implementation of the GA is organized in such a way that a single round of fitness evaluations is required for each generation. By using a multi-agent programming model for the GA, individual jobs are responsible for each evaluation of the fitness. These jobs will run in parallel on a supercalculator. This enables a very efficient parallelization of the algorithm.

3. OPTIMIZED ABSORPTION OF SOLAR RADIATIONS IN A NANO-STRUCTURED THIN FILM OF SILICON

In the context of the European project PhotoNVoltaics,[20] we seek at optimizing the absorption of solar radiation in nano-structured thin films of silicon by taking advantage of light-trapping mechanisms.[8–10] These systems must be carefully designed in order to avoid reflections of the incident radiation at the front side as well as parasitic absorption in the materials that do not contribute to the production of electricity. One of the systems addressed in this project is depicted in Fig. 1.

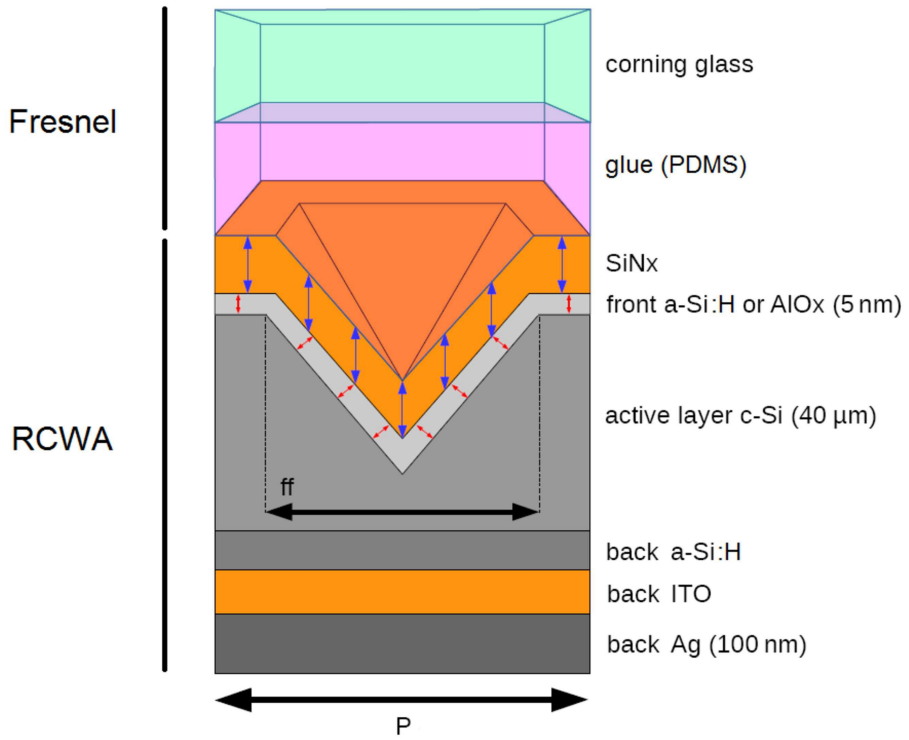

Figure 1. Photovoltaic cell whose active part consists of a thin film (40 μm) of crystalline silicon, with a periodic array of inverted pyramids on the front side. A 5-nm thick layer of a-Si:H or AlO_x is used for passivation. A conformal layer of SiN_x plays the role of anti-reflection coating. The back side includes a layer of a-Si:H for passivation. Two layers of ITO and Ag play the role of back reflector. A corning glass is finally used for encapsulation.

The active part of this photovoltaic cell consists of a thin film of crystalline silicon (c-Si), whose thickness has been limited to 40 μm. A periodic array of inverted pyramids is introduced in order to (i) reduce front-side

reflections of the incident radiation (effect essentially due to the gradual adaptation of the refractive index at the surface), and (ii) couple the incident radiation into quasi-guided modes of the corrugated film (light-trapping).[10] This array of pyramids is obtained by Nano-Imprint Lithography (NIL)[21] followed by a wet chemical etching using tetramethyl ammonium hydroxide (TMAH).[22] This etching acts preferably along the {111} crystallographic direction of silicon, so that the faces of these inverted pyramids form an angle α of 54.7° with the horizontal plane. A 5-nm thick conformal layer of amorphous silicon (a-Si:H) is deposited by PECVD for passivation purposes. A layer of SiN_x finally serves as Anti-Reflection Coating (ARC). On the rear side, a layer of a-Si:H is used for passivation. Two layers of Indium Tin Oxide (ITO) and Ag play the role of back reflector. A corning glass is finally used for encapsulation of the device. A layer of glue (PDMS) fills the gap between the corning glass and the active part of the device.

Our objective is to maximize the absorption of solar radiation in the crystalline silicon by determining optimal geometrical parameters for the device depicted in Fig. 1. Assuming a perfect collection of the electron-hole pairs generated by each photon absorbed in the active layer, the *short-circuit current* J_{sc} is given by

$$J_{\mathrm{sc}} = \frac{e}{hc} \int_{300\ \mathrm{nm}}^{1200\ \mathrm{nm}} S(\lambda) A_{\mathrm{c-Si}}(\lambda) \lambda d\lambda \,, \tag{1}$$

where e is the electron charge, h the Planck's constant, c the speed of light in vacuum, λ the wavelength in vacuum, $S(\lambda)$ the normalized AM1.5G solar irradiance spectrum and $A_{\mathrm{c-Si}}(\lambda)$ the absorption spectrum inside the corrugated crystalline silicon layer. It is understood that the efficiency $\eta = FF.J_{\mathrm{sc}}.V_{\mathrm{oc}}/\int_0^\infty S(\lambda)d\lambda$ of a real device will also depend on the capacity to collect these electron-hole pairs (FF is the *fill factor* and V_{oc} the *open-circuit voltage* of the solar cell). As demonstrated in previous work,[7,9] J_{sc} tends to increase with the c-Si thickness while V_{oc} tends to decrease. A compromise must therefore be found, which depends critically on the quality of the surface passivation. These aspects were taken into consideration when establishing the design of our solar cell and an Interdigitated Back-Contact (IBC) heterojunction cell with a c-Si thickness of 40 μm was adopted in order to deal with these electrical issues.[8,9] The current work focusses on getting a maximal optical absorption in the crystalline silicon (value reflected by the short-circuit current J_{sc}), given these experimental constraints.

The calculation of J_{sc} by Eq. (1) requires the computation of the absorbtion spectrum $A_{\mathrm{c-Si}}(\lambda)$ inside the corrugated crystalline silicon layer. We used for this purpose a hybrid Fresnel-RCWA model in which reflections of the incident radiation at the air-glass and glass-glue interfaces are taken into account by Fresnel intensity reflection coefficients.[23] This approach discards artificial interferences that appear if multiple reflections of the incident radiation between these two interfaces are described through a wave equation. These interferences give rise indeed to sharp Fabry-Perot peaks in the absorption spectrum, whose wavelength positions depend artificially on the thickness of the glass and the glue. Since these interferences are anyway smoothed out in a real device because of the macroscopic features of these layers and the finite temporal coherence length of the solar radiation,[24] it is better to discard them from the beginning in the simulations. The rest of the device is treated by a Rigorous Coupled-Waves Analysis (RCWA)[25–27] since the 40 micron thickness of the c-Si layer is still of the order of the light coherence length. This approach provides a numerically exact resolution of Maxwell's equations in the active part of the device, which has dimensions comparable to the solar radiation wavelengths. With the recent developments presented in Ref. 10, we have access to a three-dimensional mapping of the absorption inside the active part of the device and therefore to $A_{\mathrm{c-Si}}(\lambda)$. This absorption spectrum was calculated for 197 wavelengths between 300 and 1200 nm. The distribution of these wavelengths and the number of plane waves used in each case for the RCWA calculations were adapted to the different regions of the absorption spectrum. The number of plane waves was limited to 9×9 when running the genetic algorithm in order to limit computation times. The results discussed hereafter in this paper were confirmed by calculations limited this time to 11×11 plane waves in order to ensure their reliability. The $A_{\mathrm{c-Si}}(\lambda)$ absorption spectrum was interpolated on a high-resolution grid (step of 0.5 nm) by using a shape-preserving piecewise cubic interpolation method, before finally evaluating the integral in Eq. (1) by a trapezoidal rule in order to get J_{sc}. This interpolation of the $A_{\mathrm{c-Si}}(\lambda)$ spectrum on a fine grid was necessary in order to account for spectral details of the AM1.5G solar spectrum.[10]

The parameters to be determined in order to optimize J_{sc} are then (i) the period P of the square array of inverted pyramids, (ii) the area fill factor ff of these pyramids (defined as the ratio between the area of the holes

on the front side of the c-Si and the area of the periodic cell), (iii) the thickness of the SiN_x, (iv) the thickness of the back a-Si:H, and (v) the thickness of the back ITO. The range of parameters explored by the genetic algorithm is given in Table 1. Considering the granularity associated with each parameter, there is a total of 16,120,700,046 possible parameter combinations. Each fitness calculation requires up to 17 hours of cpu time. This optimization problem would therefore be untractable by traditional methods based on a systematic scan on parameters.

Table 1. Parameters to be determined by the genetic algorithm, with the range of variation and the granularity associated with each parameter.

Period P	500-1000 nm (step of 1 nm)
Area fill factor ff	50-95% (step of 1%)
Thickness of SiN_x	20-140 nm (step of 1 nm)
Thickness of back a-Si:H	10-50 nm (step of 1 nm)
Thickness of back ITO	40-180 nm (step of 1 nm)

Table 2. Parameters determined by the genetic algorithm for the optimization of optical absorption in a nanostructured thin film (40 μm) of crystalline silicon. In the first column, passivation is achieved by a 5 nm-thick layer of a-Si:H. In the second column, passivation is achieved by a 5 nm-thick layer of AlO_x. The values provided for the short-circuit current J_{sc} correspond to a Fresnel-RCWA model and a full RCWA model of the solar cell. These data were calculated with a maximum of 11×11 plane waves for the RCWA calculations.

Material used for the front-side passivation	a-Si:H	AlO_x
Period P	684 nm	697 nm
Area fill factor ff	92%	93%
Thickness of SiN_x	87 nm	70 nm
Thickness of back a-Si:H	33 nm	41 nm
Thickness of back ITO	40 nm	42 nm
J_{sc} by the Fresnel-RCWA model	37.0 mA/cm^2	39.1 mA/cm^2
J_{sc} by a full RCWA model with artificial Fabry-Perot resonances	37.4 mA/cm^2	39.6 mA/cm^2

The results found at this point by the genetic algorithm are given in Table 2. The calculations are still running at the time of writing this conference proceeding and it is therefore likely that better results will be found. These results were obtained after 30 generations of the genetic algorithm. They show that it is possible to achieve a short-circuit current J_{sc} of 37.0 mA/cm^2 with a-Si:H as front-side passivation layer by using the parameters found by the GA. This value is provided by a model in which the reflections at the air-glass and glass-glue interfaces are treated by intensity reflection coefficients. By using a full RCWA model in which the glass and the glue layers are both given arbitrarily a finite thickness of 40 μm, a value of J_{sc}=37.4 mA/cm^2 is achieved. These glass and glue thicknesses were chosen to illustrate the Fabry-Perot resonances that would appear in the $A_{c-Si}(\lambda)$ spectrum if the propagation of the incident radiation in the glass and the glue were treated through a wave equation. Therefore they are not representative of a real device. This comparison only aims at validating the Fresnel-RCWA model. The J_{sc} value provided by the full RCWA model is slightly higher than that provided by the Fresnel-RCWA model. This is due to the resonance peaks that appear in the lower part of the absorption spectrum because of multiple reflections of the incident radiation at the air-glass and glass-glue interfaces (see Fig. 2). These resonances are an artificial outcome of a full RCWA modeling in which the glass and the glue are given a finite thickness comparable with that of the c-Si (values not representative of a real device). By contrast, the sharp resonance peaks seen at longer wavelengths (above 800 nm) do have a

physical origin since they are due to quasi-guided modes in the corrugated film. The J_{sc} data used by the genetic algorithm is provided by a Fresnel-RCWA model that discards numerical artifacts (artificial interference peaks), hence providing results that will be more robust when used for the fabrication of a real device.

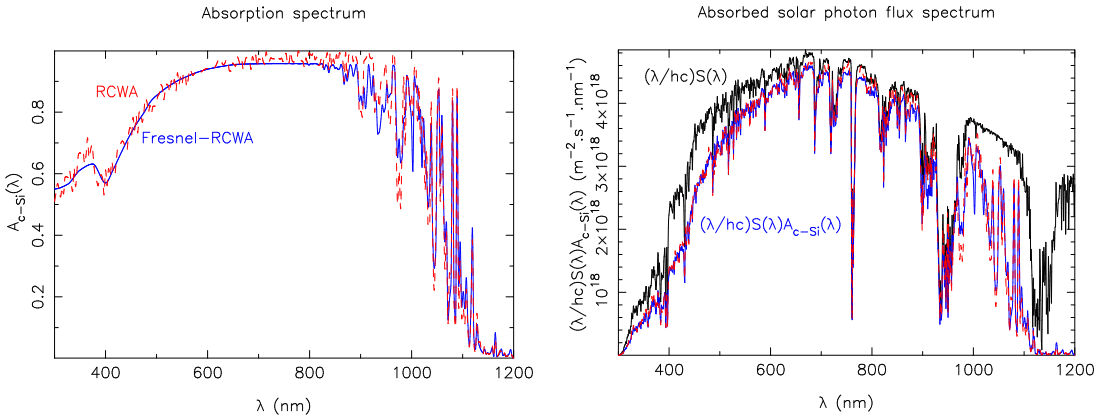

Figure 2. Left: Absorption spectrum $A_{\mathrm{c-Si}}(\lambda)$ for the parameters given in the first column of Table 2 (passivation by a-Si:H), as provided by the Fresnel-RCWA model (solid) and the full RCWA model (dashed); Right: Absorbed solar photon flux spectrum $\frac{\lambda}{hc}S(\lambda)A_{\mathrm{c-Si}}(\lambda)$ for the Fresnel-RCWA model (solid) and the full RCWA model (dashed). The figure includes the solar photon flux spectrum $\frac{\lambda}{hc}S(\lambda)$ for reference.

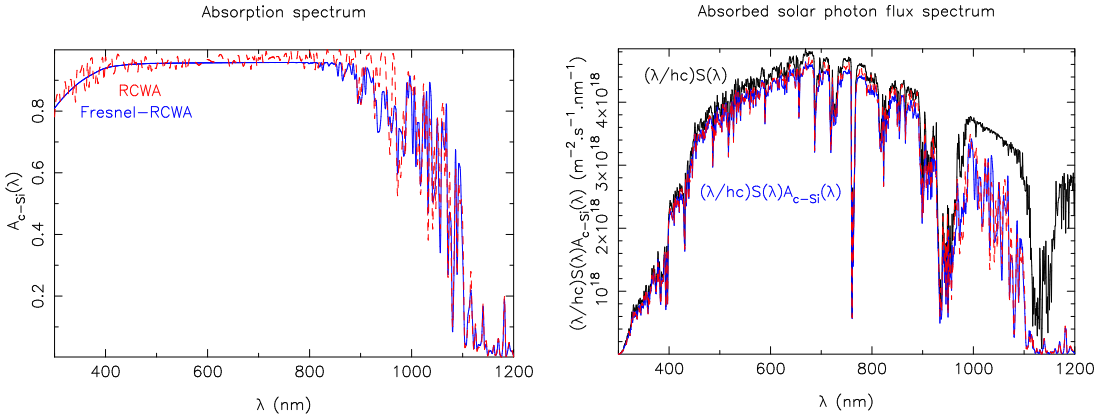

Figure 3. Left: Absorption spectrum $A_{\mathrm{c-Si}}(\lambda)$ for the parameters given in the second column of Table 2 (passivation by AlO_x), as provided by the Fresnel-RCWA model (solid) and the full RCWA model (dashed); Right: Absorbed solar photon flux spectrum $\frac{\lambda}{hc}S(\lambda)A_{\mathrm{c-Si}}(\lambda)$ for the Fresnel-RCWA model (solid) and the full RCWA model (dashed). The figure includes the solar photon flux spectrum $\frac{\lambda}{hc}S(\lambda)$ for reference.

The short-circuit currents discussed in Table 2 must be compared with the theoretical limit of 43.5 mA/cm^2 one can achieve when working with crystalline silicon. In most commercial modules, the thickness of the c-Si wafer is typically of between 150 and 200 microns. The results presented here are achieved with a c-Si thickness of 40 μm only. They are consistent with values reported by Andreani et al. for similar systems.[7] It turns out that the a-Si:H passivation layer is actually responsible for a significant absorption of the incident radiation for $\lambda < 600$ nm (see Fig. 2). This prevented us from reaching higher efficiencies. By using a transparent AlO_x instead of a-Si:H for the front-side passivation,[9,28] we can reach short-circuit currents that are much closer to 40 mA/cm^2. This is illustrated in the second column of Table 2, where the front-side passivation layer consists this time of a 5-nm thick AlO_x. A short-circuit current of 39.1 mA/cm^2 is provided by the Fresnel-RCWA model, while a value of 39.6 mA/cm^2 is achieved when working with a full RCWA model of the solar cell. The

absorption spectrum obtained with this layer of AlO_x is represented in Fig. 3. Absorption of solar radiation in the crystalline silicon turns out to be significantly enhanced for $\lambda < 600$ nm, which explains the higher values achieved for J_{sc}.

4. CONCLUSION

We used a genetic algorithm to optimize the absorption of solar radiations in a thin film of crystalline silicon for the development of high-performance photovoltaics. The solar cell considered in this work was representative of a realistic module. It involves a whole set of characteristic parameters that have to be adjusted in order to reach high efficiencies. The genetic algorithm makes it possible to address this optimization problem by evaluating only a reduced number of parameter combinations. This approach, which is based on a collective exploration of the parameter space, takes advantage of massive parallelization techniques for the evaluation of these parameters. Different heuristics were implemented in order to achieve an efficient exploration of the parameter space, while also helping the genetic algorithm in finalizing the optimization once the good spot has been found. The results provided by the genetic algorithm show that the area fill factor of the solar cell surface corrugation should be as high as experimentally possible. This parameter tends indeed to converge to its upper-boundary specification. This can be understood by the need of a reduced flat surface and a progressive index variation on the front side of the device, in order to reduce the reflection of incident radiation. A more pronounced surface corrugation also leads to a better coupling of the incident radiation with the quasi-guided modes of the crystalline silicon. The optimal cell periodicity is of the order of 700 nm, which corresponds actually to the maximum of the solar photon flux spectrum. The anti-reflection coating and the back reflector layers play their role in ensuring that a maximum of the incident radiation is indeed absorbed in the crystalline silicon. The a-Si:H front-side passivation layer turns out however to be responsible for a significant parasitic absorption of the solar radiation. When using transparent AlO_x instead of a-Si:H for the front-side passivation, short-circuit currents of 39.1 mA/cm^2 are finally achieved. This work is still in progress and further improvements are expected.

APPENDIX A. COUPLING THE GENETIC ALGORITHM WITH LOCAL OPTIMIZATIONS BASED ON A QUADRATIC FIT OF THE BEST INDIVIDUALS

Genetic Algorithms are typically slow at finalizing the optimization despite the fact substantial data around the final optimum is collected. In order to accelerate this final step of the optimization, we analyzed every five generations the data collected by the GA in order to infer the final solution from a quadratic fit of the best individuals.

The first step of this predictive heuristic consists in selecting a restricted set of points in the close vicinity of the current best solution. This selection is performed on a record that contains all individuals for which the fitness has been calculated. The selected solutions are those for which $f(\vec{x}) \geq f_{thr}$ and $s \geq 0.9$, where $f_{thr} = f_{min} + 0.9 \times (f_{max} - f_{min})$ with f_{min} and f_{max} respectively the minimal and maximal fitness values achieved in the record. s refers to the fraction of bits whose values are identical with the best individual. Different selection criteria may be adopted depending on the application. The point is that these selected individuals must all be in the close vicinity of the optimum we seek at refining.

A reference point is defined by $\vec{x}_{ref} = \sum_i \vec{x}_i f(\vec{x}_i) / \sum_i f(\vec{x}_i)$, where the sum is restricted to the points selected in the previous step. The idea consists then in establishing a quadratic fit of these points by an expression of the form

$$f(\vec{x}) = a_0 + \vec{A}_1.(\vec{x} - \vec{x}_{ref}) + \frac{1}{2}(\vec{x} - \vec{x}_{ref}).\mathbf{A}_2(\vec{x} - \vec{x}_{ref}) \,, \tag{2}$$

where a_0 is a scalar, $\vec{A}_1$ is a vector of size n and $\mathbf{A}_2$ is a symmetric matrix of size $n \times n$. This is a linear adjustment problem for the coefficients in a_0, $\vec{A}_1$ and $\mathbf{A}_2$, which can be solved easily if the number of selected points is larger than the number of coefficients.

Let us define $\vec{f}$ as a vector of size n_{select} that contains the $f(\vec{x})$ values for our selection of points and $\vec{A}$ a vector of size $n_{coeff} = 1 + n + n.(n+1)/2$ that contains the unknown coefficients in a_0, $\vec{A}_1$ and $\mathbf{A}_2$. The adjustment to achieve can be written as $\vec{f} = \mathbf{M}\vec{A}$, where $\mathbf{M}$ is a $n_{select} \times n_{coeff}$ matrix defined from Eq. (2). By using a Singular

Values Decomposition (SVD) of the matrix $\mathbf{M}$, the adjustment to achieve can be written as $\vec{f} = \mathbf{U}\mathbf{\Sigma}\mathbf{V}^t\vec{A}$, where $\mathbf{U}$ is an orthonormal matrix of size $n_{\text{select}} \times n_{\text{coeff}}$ and $\mathbf{V}$ is an orthonormal matrix of size $n_{\text{coeff}} \times n_{\text{coeff}}$. $\mathbf{\Sigma}$ is a diagonal matrix of size $n_{\text{coeff}} \times n_{\text{coeff}}$ that contains the singular values σ_i of the matrix $\mathbf{M}$.[29] The solution of our adjustment is then given by $\vec{A} = \mathbf{V}\mathbf{\Sigma}^+\mathbf{U}^t\vec{f}$, where $\mathbf{\Sigma}^+$ is a diagonal matrix of size $n_{\text{coeff}} \times n_{\text{coeff}}$ whose diagonal elements are defined by σ_i^{-1} if $\sigma_i \geq \sigma_{\max}/10^4$ (with $\sigma_{\max} = \max_i \sigma_i$) and 0 otherwise. This threshold of $\sigma_{\max}/10^4$ was chosen for numerical stability reasons. The threshold value to use may depend on the application.

Once the adjustment given in Eq. (2) has been achieved, the solution of $\vec{\nabla} f = 0$ is formally given by $\vec{x}^* = \vec{x}_{\text{ref}} - \mathbf{A}_2^{-1}\vec{A}_1$. Since in general there is no guarantee that the matrix $\mathbf{A}_2$ can be inverted, it is safer to use an approach based on the spectral decomposition of $\mathbf{A}_2$. Since the matrix $\mathbf{A}_2$ is symmetric, one can obtain $\mathbf{A}_2\vec{x}_i = \lambda_i\vec{x}_i$, where the eigenvalues λ_i are real and the eigenvectors $\vec{x}_i$ form an orthonormal basis. The solution of $\vec{\nabla} f = 0$ is then given by

$$\vec{x}^* = \vec{x}_{\text{ref}} - \sum_i \frac{\vec{x}_i.\vec{A}_1}{\lambda_i}\vec{x}_i \,, \tag{3}$$

where the sum is restricted to the eigenvalues λ_i for which $|\lambda_i| \geq \lambda_{\max}/10^2$ with $\lambda_{\max} = \max_i |\lambda_i|$ in order to avoid numerical instabilities. The threshold value to use here is may depend again on the application.

If the solution $\vec{x}^*$ provided by this approach matches all parameter specifications, we finally inject in the population an individual whose DNA codes for $\vec{x}^*$. This heuristics accelerates the refinement of the optimum once a sufficient amount of data has been collected. We use $\vec{x}_{\text{ref}}$ as prediction of the optimum if the calculation of $\vec{x}^*$ can not be completed.

ACKNOWLEDGMENTS

A.M. is funded as Research Associate by the Fund for Scientific Research (F.R.S.-FNRS) of Belgium. He is member of NaXys, Namur Center for Complex Systems, University of Namur, Belgium. This research used the Tier-1 supercalculator at Gosselies, Belgium, which received financial support from the Walloon Region and is administrated by Cenaero (http://www.cenaero.be). It also used resources of the "Plateforme Technologique de Calcul Intensif (PTCI)" (http://www.ptci.unamur.be) located at the University of Namur, Belgium, which is supported by the F.R.S.-FNRS under the convention No. 2.4520.11. The PTCI is member of the "Consortium des Equipements de Calcul Intensif (CECI)" (http://www.ceci-hpc.be). All partners (IMEC, CNRS-INL, CNRS-LPICM, Obducat, Chalmers and Total) of the European project PhotoNVoltaics are acknowledged for their contribution in the design of the solar cell considered in this work and for providing the optical data required by the simulations. Loïc Lolouat (CNRS-INL) is acknowledged for providing FDTD results that enabled validation of the RCWA code. Valerie Depauw (IMEC) is acknowledged for her critical reading of this manuscript. This project has received funding from the European Union's Seventh Framework Programme for research, technological development and demonstration under grant agreement No 309127, PhotoNVoltaics (http://www.photonvoltaics.org).

REFERENCES

[1] Singh, R., "Why silicon is and will remain the dominant photovoltaic material," *J. Nanophotonics* **3**, 032503 (2009).

[2] Luque, A., "Will we exceed 50% efficiency in photovoltaics?," *J. Appl. Phys.* **110**, 031301 (2011).

[3] Bozzola, A., Liscidini, M., and Andreani, L., "Photonic light-trapping versus lambertian limits in thin film silicon solar cells with 1d and 2d periodic patterns," *Opt. Express* **20**, A224–A244 (2012).

[4] Rothemund, R., Umundum, T., Meinhardt, G., Hingerl, K., Fromherz, T., and Jantsch, W., "Light trapping in pyramidally textured crystalline silicon solar cells using back-side diffractive gratings," *Prog. Photovoltaics* **21**, 747–753 (2013).

[5] Peretti, R., Gomard, G., Lalouat, L., Seassal, C., and Drouard, E., "Absorption control in pseudodisordered photonic-crystal thin films," *Phys. Rev. A* **88**, 053835 (2013).

[6] Ingenito, A., Isabella, O., and Zeman, M., "Experimental demonstration of $4n^2$ classical absorption limit in nanotextured ultrathin solar cells with dielectric omnidirectional back reflector," *ACS Photonics* **1**, 270–278 (2014).

[7] Andreani, L., Bozzola, A., Kowalczewski, P., and Liscidini, M., "Photonic light trapping and electrical transport in thin-film silicon solar cells," *Sol. Energ. Mat. Sol. C.* **135**, 78–92 (2015).

[8] Trompoukis, C., Abdo, I., Cariou, R., Cosme, I., Chen, W., Deparis, O., Dmitriev, A., Drouard, E., Foldyna, M., Garcia-Caurel, E., Gordon, I., Heidari, B., Herman, A., Lalouat, L., Lee, K.-D., Liu, J., Lodewijks, K., Mandorlo, F., Massiot, I., Mayer, A., Mijkovic, V., Muller, J., Orobtchouk, R., Poulain, G., Prod'Homme, P., Roca i Cabarrocas, P., Seassal, C., Poortmans, J., Mertens, R., El Daif, O., and Depauw, V., "Photonic nanostructures for advanced light trapping in thin crystalline silicon solar cells," *Phys. Status Solidi A* **212**, 140–155 (2015).

[9] Depauw, V., Abdo, I., Boukhicha, R., Cariou, R., Chen, W., Bolanos, I., Deparis, O., Ding, H., Dmitriev, A., Drouard, E., El Daif, O., Fave, A., Foldyna, M., Garcia-Caurel, E., Heidari, B., Herman, A., Lalouat, L., Lee, K., Liu, J., Lodewijks, K., Mandorlo, F., Massiot, I., Mayer, A., Muller, J., Narchi, P., Orobtchouk, R., Picardi, G., Prod'Homme, P., Roca i Cabarrocas, P., Seassal, C., Trompoukis, C., Gordon, I., and Poortmans, J., "Nanophotonics for ultra-thin crystalline silicon photovoltaics: when photons (actually) meet electrons," *EU PVSEC Proceedings* **29**, 1461–1469 (2014).

[10] Muller, J., Herman, A., Mayer, A., and Deparis, O., "A fair comparison between ultrathin crystalline-silicon solar cells with either periodic or correlated disorder inverted pyramid textures," *Opt. Express* **23**, A657–A670 (2015).

[11] Boden, S. and Bagnall, D., "Sunrise to sunset optimization of thin film antireflective coatings for encapsulated, planar silicon solar cells," *Prog. Photovoltaics* **17**, 241–252 (2009).

[12] Oh, S., Chhajed, S., Poxson, D., Cho, J., Schubert, E., Tark, S., Kim, D., and Kim, J., "Enhanced broadband and omni-directional performance of polycristalline Si solar cells by using discrete multilayer antireflection coatings," *Opt. Express* **21**, A157–A166 (2013).

[13] Holland, J., [*Adaptation in Natural and Artificial Systems*], University of Michigan Press, Ann Arbor, Mich. (1975).

[14] De Jong, K., [*An Analysis of the Behaviors of Genetic Adaptative Systems*], PhD thesis, University of Michigan, Ann Arbor, Mich. (1975).

[15] Goldberg, D., [*Genetic Algorithms in Search, Optimization and Machine Learning*], Addison-Wesley, Reading, Mass. (1989).

[16] Judson, R., "Genetic algorithms and their use in chemistry," *Reviews in Computational Chemistry* **10**, 1–73 (1997).

[17] Haupt, R. and Werner, D., [*Genetic Algorithms in Electromagnetics*], J. Wiley & Sons, Hoboken, NJ (2007).

[18] Eiben, A. and Smith, J., [*Introduction to Evolutionary Computing*], Springer-Verlag, Berlin, second ed. (2007).

[19] Mayer, A. and Bay, A., "Optimization by a genetic algorithm of the light-extraction efficiency of a GaN light-emitting diode," *J. Optics* **17**, 025002 (2015).

[20] European Project PhotoNVoltaics. http://www.photonvoltaics.org.

[21] Chou, S., Krauss, P., and Renstrom, P., "Imprint of sub-25 nm vias and trenches in polymers," *Appl. Phys. Lett.* **67**, 3114–3116 (1995).

[22] Frühauf, J., [*Shape and Functional Elements of the Bulk Silicon Microtechnique: a Manual of Wet-Etched Silicon Structures*], Springer-Verlag, Berlin (2005).

[23] Jackson, J., [*Classical Electrodynamics*], J. Wiley & Sons, New York, third ed. (1999).

[24] Herman, A., Sarrazin, M., and Deparis, O., "The fundamental problem of treating light incoherence in photovoltaics and its practical consequences," *New J. Phys.* **16**, 013022 (2014).

[25] Vigneron, J.-P., Forati, F., André, D., Castiaux, A., Derycke, I., and Dereux, A., "Theory of electromagnetic energy transfer in three-dimensional structures," *Ultramicroscopy* **61**, 21–27 (1995).

[26] Vigneron, J.-P. and Lousse, V., "Variation of a photonic crystal color with the Miller indices of the exposed surface," in [*Photonic Crystal Materials and Devices IV*], Adibi, A., Lin, S.-Y., and Scherer, A., eds., *Proc. SPIE* **6128**, 61281G (2006).

[27] Brenner, K.-H., "Aspects for calculating local absorption with the rigorous coupled-wave method," *Opt. Express* **18**, 10369–10376 (2010).

[28] Savin, H., Repo, P., von Gastrow, G., Ortega, P., Calle, E., Garin, M., and Alcubilla, R., "Black silicon solar cells with interdigitated back-contacts achieve 22.1% efficiency," *Nat. Nanotechnol.* **10**, 624–628 (2015).

[29] Golub, G. and Kahan, W., "Calculating the singular values and pseudo-inverse of a matrix," *J. Soc. Ind. Appl. Math. Ser. B Numer. Anal.* **2**, 205–224 (1965).